Persistent spectral hole burning and water content in Eu^{3+}-doped aluminosilicate glasses

Masayuki Nogami†, Takehito Nagakura and Tomokatsu Hayakawa

Nagoya Institute of Technology, Showa Nagoya 466-8555, Japan

Abstract. Persistent spectral hole burning (PSHB) was investigated in Eu^{3+}-doped Al$_2$O$_3 \cdot$9SiO$_2$ glass prepared by the sol–gel method. The hole was burned in the ^{7}F$_0 \rightarrow$ ^{5}D$_0$ line of the Eu^{3+} ions using a rhodamine 6G dye laser at 77 K, the hole area of which was proportionally increased with the content of OH groups surrounding the Eu^{3+} ions. The local environment of the Eu^{3+} ions in glass was examined from the fluorescence line narrowing spectra of the ^{5}D$_0 \rightarrow$ ^{7}F$_1$ transition. The three splitting energies of the ^{7}F$_1$ level diverged with the increase of the excitation energy. It was concluded that the PSHB was formed by optically changing the bonding feature of proton in the coordinating sphere of the Eu^{3+} ions into the activated state, the barrier height of which was estimated as 0.3 eV.

1. Introduction

Rare-earth-ion-doped glasses have attracted great attention, because they show a high temperature persistent spectral hole burning (PSHB) [1, 2] and have a large potential for a high-density frequency-domain optical data memory [3]. We have been conducting a study of the preparation of the PSHB glasses by use of a sol–gel technique, and succeeded in preparing Sm^{2+}-doped aluminosilicate glasses exhibiting PSHB up to room temperature [4–6]. The samarium ions are generally incorporated as the trivalent state in glasses, and are reduced into Sm^{2+} by heating in an H$_2$ gas atmosphere. More recently, we reported for the first time to our knowledge that the Eu^{3+}-ion-doped silica glass prepared by the sol–gel method exhibited PSHB up to 130 K [7]. Since the Eu^{3+}-doped glasses are obtained without heating in a reducing atmosphere, it thus becomes possible to extend the study beyond the limitations of the Sm^{2+}-doped glasses. In a previous paper, we found that the hole-depth proportionally increased as the residual water content increased [8], and proposed that the hole is formed by the concerted action of OH bonds in the first coordination sphere surrounding the Eu^{3+} ions. This hole-burning mechanism is different from that of the Sm^{2+} ions, where the photoionization of Sm^{2+} into Sm^{3+} by laser irradiation is the main reaction. Our further research was successful in preparation of the Eu^{3+}-doped aluminosilicate glasses exhibiting PSHB up to 200 K, which was by 70 K higher than that of silica glass [9]. These results suggest that the hole burning of the Eu^{3+}-doped glasses is strongly affected by the glass composition and the OH content. The search for hole burning in the Eu^{3+}-doped glasses is important for the development of glasses exhibiting PSHB at high temperature.

The aim of this work is a detailed study of the hole burning of the Eu^{3+}-doped Al$_2$O$_3$–SiO$_2$ glasses prepared by the sol–gel technique. Hole-burning properties are discussed to be related

† Corresponding author. E-mail address: `nogami@mse.nitech.ac.jp`.

with the water content in glasses. The local structure around the Eu^{3+} ions is studied using the fluorescence line narrowing technique.

2. Experimental methods

2.1. Sample preparation

$Al_2O_3 \cdot 9SiO_2$ (mole ratio) glass containing nominally 2 wt% Eu_2O_3 was prepared by the hydrolysis of $Si(OC_2H_5)_4$, $Al(OC_4H_9^{sec})_3$ and $Eu(NO_3)_3 \cdot 6H_2O$. The starting materials were commercially available and used as received. The $Si(OC_2H_5)_4$ was first hydrolysed for 1 h at room temperature with a mixed solution of H_2O, C_2H_5OH and HCl in the molar ratios of 1:1:0.0027 per mole of $Si(OC_2H_5)_4$. $Al(OC_4H_9^{sec})_3$ was added in this solution, followed by stirring for 15 min at 70 °C. After cooling to room temperature, $Eu(NO_3)_3 \cdot 6H_2O$ dissolved in C_2H_5OH was added and stirred for 1 h. The resulting homogeneous solution was finally hydrolysed with H_2O, C_2H_5OH and HCl. In this second reaction, the molar ratio was maintained at 4:1:0.011 per mole of metal alkoxide. After the solution had been stirred for 1 h, it was left for about 2 weeks to form a stiff gel about 2 mm thick. The dried gel was heated to 150 °C in a tightly sealed vessel together with water and held for 15 h in order to completely hydrolyse the alkoxides. The resulting gel was heated in air at 50 °C h^{-1} to 400–1000 °C and held at that temperature for 2 h.

2.2. Measurements of hole-burning and fluorescence spectra

The PSHB was observed on the excitation spectrum of the $^7F_0 \rightarrow {}^5D_0$ transition of the Eu^{3+}. The excitation spectrum was obtained by scanning the output of a cw Ar^+ ion laser-pumped rhodamine 6G dye laser with a linewidth of ~ 1.0 cm^{-1} full width at half maximum (FWHM) from 17 100 to 17 500 cm^{-1} while monitoring the luminescence of the $^5D_0 \rightarrow {}^7F_2$ transition at 16 260 cm^{-1}. The glass was then irradiated using rhodamine 6G dye laser with a spot size of about 1 mm diameter operating at 400 mW for 30 min. After irradiation, the excitation spectrum was recorded in the same way. The laser power for scanning was attenuated by neutral density filters to less than 0.2% of that for burning. The luminescence spectra were recorded at room temperature. The 25 380 cm^{-1} light of an Xe lamp was used as a pumping source, which matched the $^7F_0 \rightarrow {}^5L_6$ transition of the Eu^{3+}. For the luminescence lifetime measurements, an N_2-laser-pumped DPS dye laser was focused onto the sample and the luminescence at 16 260 cm^{-1} wavelength was recorded using a CCD camera. The fluorescence line narrowing (FLN) measurement was performed under excitation with a wavelength within the $^7F_0 \rightarrow {}^5D_0$ transition using a rhodamine 6G dye laser. The luminescence intensity was measured with a chopper that alternately opened the optical paths before and after the sample. The chopping frequency was 150 Hz. All FLN spectra were recorded at 77 K with the Jobin Yvon HR 320 monochromator.

The water in the glass was determined from absorption intensity of infrared (IR) spectra. IR spectra were obtained between 4000 and 2000 cm^{-1} for the ~ 0.1 mm thick sample.

3. Results and discussion

3.1. Hole burning

The Eu^{3+} ion has $4f^6$ electron configuration, the lowest and first excited states of which are $^7F_0$ and $^5D_0$, respectively. Holes were burned by irradiating the laser with the wavelength around the peak position of the $^7F_0 \rightarrow {}^5D_0$ band. Figure 1 shows typical hole spectra, burned and

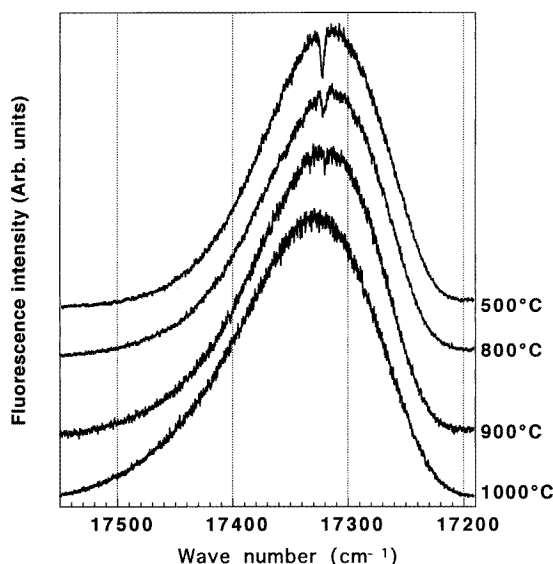**Figure 1.** Hole-burning spectra, burned and measured at 77 K, of the Eu^{3+} ion-doped Al$_2$O$_3$·9SiO$_2$ glasses obtained by heating at 500, 800, 900 and 1000 °C for 2 h. Holes were burned by means of a laser with a power of 400 mW for 30 min at 17 322 cm^{-1}.

measured at 77 K, of glasses obtained by heating at 500, 800, 900 and 1000 °C. Note that holes are clearly observed at the burning wavenumber of 17 322 cm^{-1} except for the sample heated at 1000 °C. The width and depth of the burned hole are ~1.8 cm^{-1} and ~15% of the total luminescence intensity, respectively, for the glass heated at 500 °C. We could burn the holes at wavenumber from 17 250 to 17 450 cm^{-1} covering a range of the ^{7}F$_0 \rightarrow$ ^{5}D$_0$ transition by using the laser beam with a different wavelength. The inhomogeneous width of the ^{7}F$_0 \rightarrow$ ^{5}D$_0$ transition is estimated as 125 cm^{-1} FWHM, which slightly increases as the heat-treatment temperature increases. It is interesting to notice that the hole depth is the largest for the glass heated at 500 °C and becomes smaller as the heat-treatment temperature increases. No hole is observed in the glass heated at 1000 °C or above. The characteristics of this hole-burning behaviour are consistent with the result observed in the Eu^{3+}-doped SiO$_2$ glasses [7].

3.2. Water content

Gels synthesized through the hydrolysis of metal alkoxides are porous and contain a large amount of water incorporated during gel synthesis. The water in the gel is divided into four types: physically and chemically adsorbed waters in pores, surface OH groups bonded with Si^{4+}, Al^{3+} and Eu^{3+} ions and finally OH bonds surrounded with glass network structure. The removal of physically adsorbed water in pores starts from 100 °C, followed by the removal of water molecules bound with the surface OH groups up to about 400 °C. On further heating, a dehydration–condensation reaction takes place between the surface OH groups. The porous structure remains unchanged in glasses heated below 1000 °C, at which temperature the porous glasses transform into nonporous ones by the viscous flow of gel, and some OH groups are trapped in the glass network. Characteristic of this sol–gel-derived glasses is the fact that a large amount of water is resided in glass compared with that of the glasses prepared by the conventional melt-quenching method.
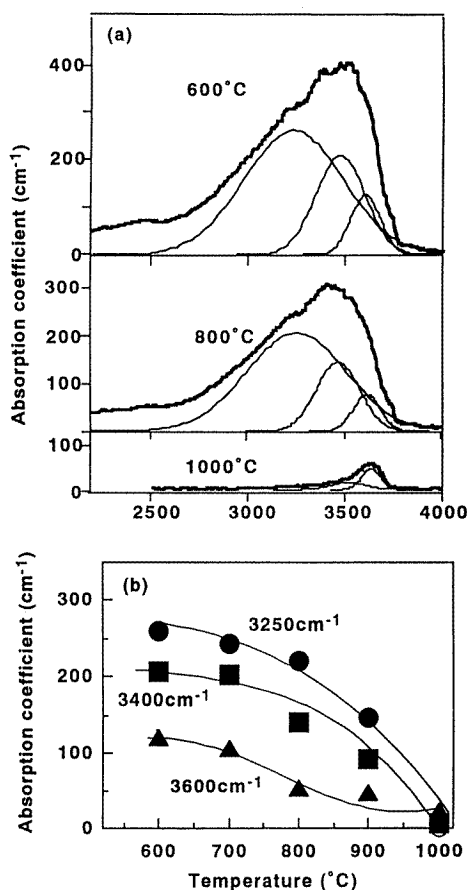
Figure 2. Infrared spectra (a) of the Eu^{3+}-ion-doped $Al_2O3 \cdot 9SiO_2$ glasses heated at 600, 800 and 1000 °C for 2 h. Spectra are deconvoluted using a Gaussian equation into three bands peaking at 3600, 3400 and 3250 cm^{-1}, the intensities of which are plotted as a function of the heat-treatment temperature (b).

To clarify the OH bonds in glasses, the IR spectra of glasses heated at 500–1000 °C were measured between 4000 and 2000 cm^{-1}. Among them, the spectra for glasses heated at 600, 800 and 1000 °C are shown in figure 2(a). Broad absorption band which is assigned to the fundamental stretching vibrations of OH groups is observed at around 3500 cm^{-1} with a shoulder at the low-wave-number side. The position of the OH-absorption bands depends on the degree of association to neighbouring oxygen through hydrogen bonding, and is shifted to low wavenumber with increasing strength of the hydrogen bonding [10, 11]. The broad absorption spectrum is deconvoluted into three bands at 3600, 3400 and 3250 cm^{-1} using a Gaussian function as shown in figure 2(a). Among the three bands, the 3600 cm^{-1} band is assigned to the hydrogen-bonding free OH groups bound with the Si^{4+} ions [11]. The presence of modifier ions in silicate glasses leads to the appearance of bands at low-wave-number regions. Therefore, the broad band at 3400 and 3250 cm^{-1} can be attributed to the OH groups bound with the Eu^{3+} and/or Al^{3+} ions through hydrogen bonding. The absorption coefficients of the deconvoluted three bands are plotted in figure 2(b) as a function of the heat-treatment temperature. It is apparent that the intensities of the bands at 3400 and 3250 cm^{-1} rapidly

decrease with increasing temperature, whereas the intensity of the 3600 cm^{-1} band is less sensitive to the temperature, indicating that the OH groups bound with the Eu^{3+} and/or Al^{3+} ions are preferentially liberated during heating at 600–1000 °C.

3.3. Fluorescence properties

The luminescence spectra, measured by using a Xe 25 380 cm^{-1} excitation wavelength, show four luminescence lines at 17 240, 16 950, 16 260 and 15 380 cm^{-1} in the visible wavelength region, all of which are assigned to the $^5D_0 \rightarrow {}^7F_j$ ($j = 0$, 1, 2, 3) transitions, respectively, of the Eu^{3+} ions. Figure 3 shows the integrated FL intensity and the decay rate of the $^5D_0 \rightarrow {}^7F_2$ transition as a function of the heat-treatment temperature. It was found that the luminescence decay curves for determining the 1/e-decay time were exponential within errors of measurement. It is well known that the presence of OH groups surrounding the Eu^{3+} ions provides an effective pathway for the radiationless deexcitation via energy transfer to OH vibration, which results in quenching the luminescence [12, 13]. Heating the glass at high temperature decreases the OH concentration and results in an increase of both the intensity and lifetime of the Eu^{3+} ions.
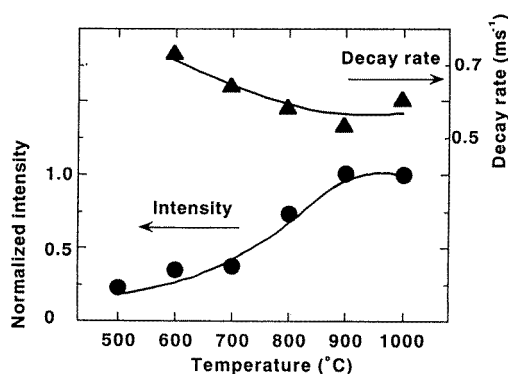

Figure 3. Luminescence intensity and decay rate as a function of heat-treatment temperature of glass. The luminescence intensity of the $^5D_0 \rightarrow {}^7F_2$ transition is normalized to unity for glass heated at 1000 °C.

The FLN spectroscopy is the most commonly used technique for studying the local environment around the Eu^{3+} ion. Figure 4 shows the FLN spectra of the $^5D_0 \rightarrow {}^7F_1$ and $^5D_0 \rightarrow {}^7F_2$ transitions of Eu^{3+}, for the sample heated at 800 °C, at 77 K under the site selective $^7F_0 \rightarrow {}^5D_0$ excitation. The $^5D_0 \rightarrow {}^7F_1$ transition is clearly structured into three distinct bands due to the Stark splitting of the $^7F_1$ state, whereas the $^5D_0 \rightarrow {}^7F_2$ transition is not well resolved. The $^7F_2$ state should be split into five components. However, the observed $^5D_0 \rightarrow {}^7F_2$ profile seems to be more complicated showing enhanced luminescence intensities on the low-energy side with increasing excitation energy, which makes any fitting procedure difficult. These phenomena suggest the existence of more components in the chemical bonds surrounding the Eu^{3+} ions. Because of this difficulty, only the $^7F_1$ Stark levels are considered in the following discussion. The difference in energy between the positions of an individual component and the excitation energy is plotted in figure 5 as a function of excitation energy in the glasses heated at 500, 800 and 1000 °C. The values determined for glasses heated at other temperatures (not plotted for clarity) are similar to those shown in figure 5. Since the $^7F_0 \rightarrow {}^5D_0$ excitation energy is a measure of the strength of the crystal field acting on central Eu^{3+} ions, such a
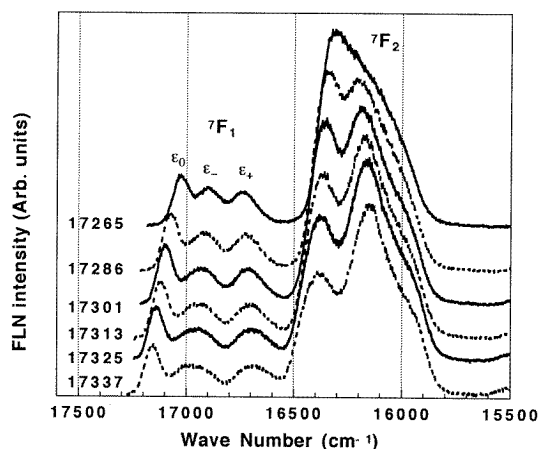
Figure 4. Fluorescence line narrowing spectra, measured at 77 K under dye-laser excitation into the $^7F_0 \rightarrow\ ^5D_0$ transition line, of the $^5D_0 \rightarrow\ ^7F_1$ and $^5D_0 \rightarrow\ ^7F_2$ transitions of Eu^{3+} ion in glass heated at 800 °C for 2 h. Numbers indicate the wavenumber of the excitation laser beam.
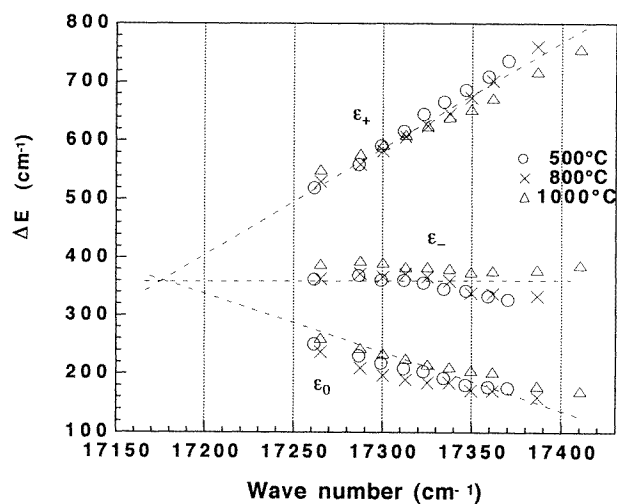

Figure 5. Energy difference between the position of the individual components of the $^5D_0 \rightarrow\ ^7F_1$ transition and the excitation wavenumber of Eu^{3+} ion in glasses heated at 500, 800 and 1000 °C as a function of the excitation wavenumber.

spectral shift can be attributed to the variation of the local crystal field strength of the Eu^{3+} ions in glass [14]. Among the three lines, the lowest-energy line shifts remarkably to lower energies with increase of the $^7F_0 \rightarrow\ ^5D_0$ excitation energy, while the other two lines shift to higher energies. The three lines seem to converge to a triply degenerate point at 340 cm^{-1} on the low energy side of 17 170 cm^{-1} and diverge with the increase of the excitation energy. These results suggest that the Eu^{3+} ions located in sites with a high symmetry at low excitation energy are changed to a low-symmetry component with the increase of the excitation energy. This behaviour of the three $^5D_0 \rightarrow\ ^7F_1$ lines is similar to that reported for the Eu^{3+}-doped silicate, borate, phosphate and fluoride glasses [14–20]. At present, we assume that the Eu^{3+}
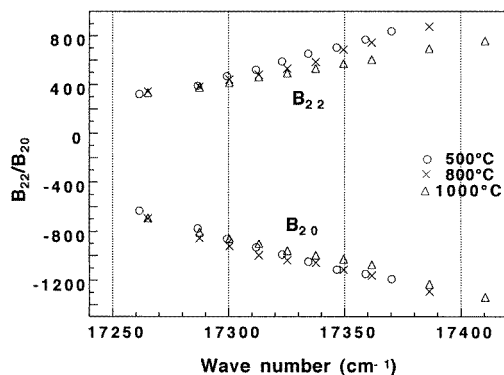
Figure 6. Second-order crystal field parameters, B_{22} and B_{20}, of glasses heated at 500, 800 and 1000 °C as a function of the excitation wavenumber.

ions have the C_{2v} symmetry as in other glasses and the three splitting energies are denoted as ε_+, ε_- and ε_0 in order of increasing energy, respectively. The component ε_0 has a large electron distribution in the z-axis and the other ε_- and ε_+ components along the $x-y$ plane [14]. Under these conditions, we can calculate the second-order crystal field parameters, B_{20} and B_{22}, for the z-axial and $x-y$ plane components, respectively, which give a more quantitative information on the local environment of the Eu^{3+} ions. The calculated second-order crystal field parameters, B_{20} and B_{22}, are plotted in figure 6 as a function of excitation energy. It is apparent that the B_{20} value decreases as the excitation energy increases, while the B_{22} value increases with the excitation energy. This suggests that oxygens surrounding the centred Eu^{3+} ion are distorted to decrease the distance between the Eu^{3+} and oxygen. On the other hand, not much difference is observed in the B_{20} and B_{22} values for the glasses obtained by heating at different temperatures between 500 and 1000 °C.

3.4. Hole properties and OH content

In the previous paper, we measured the hole depth in the Eu^{3+}-doped SiO$_2$ glasses as a function of the OH content and concluded that the hole depth increased with increasing OH content [8]. This discussion can be adapted to the present Eu^{3+}-doped Al$_2$O$_3$–SiO$_2$ glasses. To elucidate the question of which OH groups contribute to the hole burning, the relation between the hole depth and water content were plotted. Among them, a linear relation was satisfied between the hole area and the total absorption coefficients of the 3400 and 3250 cm^{-1} bands, as shown in figure 7, in which the hole area is defined as the ratio of the hole area to the total area of the $^7F_0 \rightarrow {}^5D_0$ excitation band. This result indicates that the presence of OH groups bound with the Eu^{3+} and/or Al^{3+} ions is important for the hole burning. When the laser with an energy equal to the hydrogen bonding is irradiated, the protons in the OH groups bound with Eu^{3+} and AlOH bonds surrounding Eu^{3+} change their positions to form a different bonding feature. This rearrangement of the proton bonding should result in hole burning. The hole-burnt state has a higher energy than the unburnt state and it relaxes across the activation barrier into the unburnt state.

To study the stability of the hole, hole-erasure measurements were performed at 77 K for the glass obtained by heating at 500 °C. The PSHB spectra were recorded after the burning laser is removed, the hole area of which is normalized to unity at 5 min after burning and plotted in figure 8 as a function of time with logarithmic scale. It is obvious that the hole area
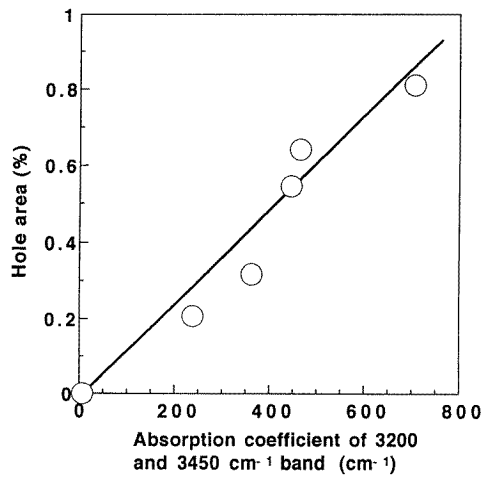
Figure 7. Hole area as a function of the total absorption coefficients of 3400 and 3250 cm^{-1} bands.
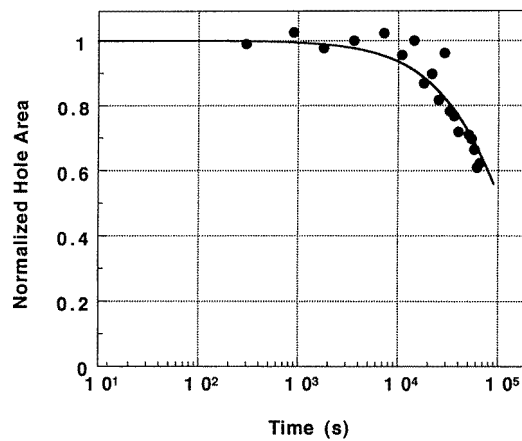

Figure 8. Hole area as a function of the time after burning laser is removed. Hole area is normalized to unity at 5 min after burning.

nonexponentially decreases with time. Such time dependence of the hole erasure is similar to those observed in the disordered materials doped with Sm^{2+} and Eu^{3+} ions, which are interpreted by a thermally activated model [21, 22]. According to this model, the fraction, HA, of the remaining hole at time, t, after removing the laser beam is a measure of the fraction of the photoproducts whose activation barriers are higher than a critical barrier height, V, and given by

$$\text{HA}(t) = \int_{-\infty}^{+\infty} g(V) \exp(-Rt) \, dV \tag{1}$$

where R is the relaxation rate of the hole and written as

$$R = R_0 \exp(-V/kT). \tag{2}$$

Assuming that the barrier height has a Gaussian distribution and the attempt frequency, R_0, is equal to the frequency of OH vibration energy (1×10^{14} s^{-1}), the data were fitted by

using equation (1), which is shown in the solid curve in figure 8, where the average thermal activation energy is estimated to be 0.29 eV. This value is close to the barrier height obtained by thermally activated recovery experiments [8], strongly suggesting that the hole burning in the Eu^{3+}-doped Al$_2$O$_3$–SiO$_2$ glasses is caused by the photoactivated rearrangement of protons in the first coordinating sphere of Eu^{3+} ions. In the course of our studies, we also observed that the glass heated at high temperature exhibited larger activation energy than that heated at low temperature.

4. Summary

We found that in the sol–gel-derived Eu^{3+}-doped Al$_2$O$_3$ · 9SiO$_2$ glasses a hole was burned by the optically activated rearrangement of the OH bonds surrounding the Eu^{3+} ions and the depth and area of the hole was proportionally increased with increasing the OH content in the glass. The holes burnt at 77 K was refilled with increasing time by the back-reaction of the OH bonds surrounding the Eu^{3+} ions.

Acknowledgments

References

[1] Hirao K, Todoroki S, Cho D H and Soga N 1993 *Opt. Lett.* **18** 1586
[2] Kurita A and Kushida T 1994 *Opt. Lett.* **19** 314
[3] Castro G, Haarer D, Macfarlane R M and Trommsdorff H P 1978 *US Patent* 4101976
[4] Nogami M and Abe Y 1994 *Appl. Phys. Lett.* **64** 1227
[5] Nogami M, Abe Y, Hirao K and Cho D H 1995 *Appl. Phys. Lett.* **66** 2952
[6] Nogami M and Abe Y 1997 *Phys. Rev.* B **56** 182
[7] Nogami M and Abe Y 1997 *Appl. Phys. Lett.* **71** 3465
[8] Nogami M and Hayakawa T 1997 *Phys. Rev.* B **56** R14 235
[9] Nogami M and Abe Y 1998 *J. Opt. Soc. Am.* B **15** 680
[10] Abe Y, Hosono H, Ohta Y and Hench L L 1988 *Phys. Rev.* B **38** 10 106
[11] Scholze H 1959 *Glasstech. Ber.* **32** 142
[12] Yan Y, Faber A J and deWaal H 1996 *J. Non-Cryst. Solids* **181** 283
[13] Nogami M and Abe Y 1996 *J. Non-Cryst. Solids* **197** 73
[14] Brecher C and Riseberg L A 1976 *Phys. Rev.* B **13** 81
[15] Nishimura G and Kushida T 1988 *Phys. Rev.* B **37** 9075
[16] Tanaka M and Kushida T 1994 *Phys. Rev.* B **49** 16 917
[17] Brecher C and Riseberg L A 1980 *Phys. Rev.* B **21** 2607
[18] Belliveau T F and Simkin D J 1989 *J. Non-Cryst. Solids* **110** 127
[19] Schmidt T H, Macfarlane R M and Volker S 1994 *Phys. Rev.* B **50** 15 707
[20] Capobianco J A, Proulx P P, Bettinnelli M and Negrosolo F 1990 *Phys. Rev.* B **42** 5936
[21] Jiahua Z, Shihua H and Jiaqi Y 1992 *Opt. Lett.* **17** 1146
[22] Yugami H, Yagi R, Matsuo S and Ishigame M 1996 *Phys. Rev.* B **53** 8283